

Do biological molecular machines act as Maxwell's demons?

Michał Kurzynski and Przemysław Chelminiak

Faculty of Physics, A. Mickiewicz University, Umultowska 85, 61-614 Poznań, Poland

(Dated: November 9, 2018)

We show that the generalized fluctuation theorem with entropy reduction is fulfilled only for the enzymatic molecular machines with the stochastic dynamics that offers a possibility of choice of the work performance in variety of ways. The particular model of such a dynamics is investigated, described by the network displaying, like networks of the systems biology, a transition from the fractal organization on a small length-scale to the small-world organization on the large length-scale. For this model the output operating flux of the machine can surpass in a natural way the input flux. The main conclusion of the study is that the energy processing has to be distinguished from the organization processing. From a broader biological perspective, three suppositions could be of especial importance: (i) a possibility of the choice is characteristic for many intrinsically disordered proteins, (ii) the tight coupling between both fluxes results not from the lack of slippage, but from the compensation of the entropy production by the information creation, and (iii) this is the reason for most protein machines to operate as dimers or higher organized structures.

PACS numbers: 05.70.Ln, 87.15.H-, 87.15.Ya, 89.75.Hc

I. INTRODUCTION

In the intention of its creator [1], Maxwell's demon was thought to be an intelligent being, able to perform work at the expense of the entropy reduction of a closed operating system. The perplexing notion of the demon's intelligence was formalized in terms of memory and information processing by Szilard [2] and subsequent followers [3, 4], who pointed out that, in order for the total system to obey the second law of thermodynamics, the entropy reduction should be compensated for by, at least, the same entropy increase, related to the demon's information gain on the operating system's state. A non-informational formulation of the problem was proposed by Smoluchowski [5] and popularized by Feynman [6] as the ratchet and pawl machine, which can operate only in agreement with the second law. A. F. Huxley [7] and consequent followers [8] adopted this way of thinking to suggest numerous ratchet mechanisms for the protein molecular machines' action, but here we show that no entropy reduction takes place for these models.

More general models of protein dynamics have been put forward [9–18] with a number of intramolecular states organized in a network of stochastic transitions. Here we show that for such models, when allowing work performance in a variety of ways [18], the generalized fluctuation theorem [19, 20] is fulfilled with possible entropy reduction. The hypothetical computer model of the network is investigated, displaying, like networks of the systems biology, a transition from the fractal organization on a small length-scale to the small-world organization on the large length-scale [21].

II. STATIONARY ISOTHERMAL MACHINES

The biological molecular machines are proteins that operate under isothermal conditions and, thus, are re-

ferred to as free energy transducers [22]. We understand the word 'machine' generally as denoting any physical system that enables two other systems to perform work on each other. The energy processing pathways in any stationary machine, that operates under isothermal conditions [23], are shown in Fig. 1, where the notation of the physical quantities being in use is also explained.

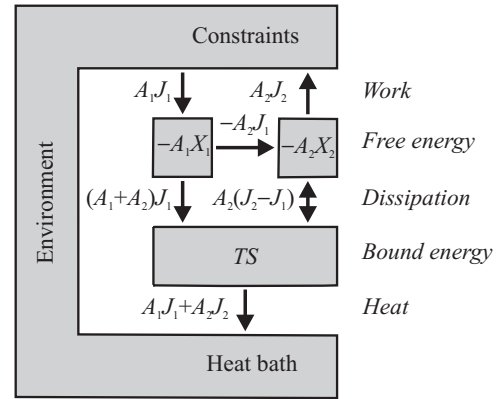


FIG. 1. Energy processing in the stationary (cyclic) isothermal machine. X_i denotes the input ($i = 1$) and the output ($i = 2$) thermodynamic variable (mechanical – displacement, electrical – charge, or chemical – number of given molecules), A_i is the conjugate thermodynamic force (mechanical force, difference of electrical or chemical potentials) and the time derivative, $J_i = dX_i/dt$, is the corresponding flux (velocity, electrical or chemical current intensity). T is the temperature and S is the entropy. The constraints keep fixed values of the thermodynamic variables. We assume these variables to be dimensionless, hence the forces are of energy dimension. By convention, we assume also the fluxes J_1 and J_2 to be of the same sign. Then, one system performs work on the other when the forces A_1 and A_2 are of the opposite sign. The directions of the energy fluxes shown are for $J_1, J_2, A_1 > 0$ and $A_2 < 0$. The direction of the flux, denoted by the forward-reverse arrow, is the subject of this research.

According to the second law of thermodynamics, the net dissipation flux (the internal entropy production rate, multiplied by the temperature) $A_1 J_1 + A_2 J_2$ must be non-negative. However, it consists of two components. The first component, $(A_1 + A_2)J_1$, realized when the input and output fluxes are tightly coupled and $J_1 = J_2$, must also be, according to the same law, nonnegative. For the present considerations, the sign of the complement $A_2(J_2 - J_1)$ is essential.

In the macroscopic systems, the entropy S is additive and can always be divided into the following two parts S_1 and S_2 , relating to the input and output thermodynamic variables X_1 and X_2 , respectively. As a consequence, the flux $A_2(J_2 - J_1)$, which corresponds to S_2 , must also be nonnegative. This means that, for negative A_2 , output flux J_2 should not surpass input flux J_1 . Macroscopically, the second component of the dissipation flux has the obvious interpretation of a slippage in the case of the mechanical machines, a leakage in the case of pumps, or a short-circuit in the case of the electrical machines. However, because of nonvanishing correlations, in the mesoscopic systems like the protein molecular machines, entropy is not additive [20], and the output flux J_2 can surpass the input flux J_1 [18], which changes the sign of the flux $A_2(J_2 - J_1)$ to the negative. Such a surprising case was observed by Yanagida and his co-workers [24, 25], who found that the single myosin II head can take several steps along the actin filament per ATP molecule hydrolyzed.

III. CHEMO-CHEMICAL MACHINES

The relation between the output and input fluxes in biological molecular machines was the topic of our previous studies [17, 18]. From a theoretical point of view, it is convenient to treat all biological machines, including molecular motors too, as chemo-chemical machines [23]. In fact, the external load influences the free energy involved in binding the motor to its track, which can be expressed as a change in the effective concentration of this track [10, 17, 23]. The chemo-chemical machines are enzymes, that simultaneously catalyze two effectively unimolecular reactions: the free energy-donating input reaction $R_1 \leftrightarrow P_1$ and the free energy-accepting output reaction $R_2 \leftrightarrow P_2$. The system considered consists of a single enzyme macromolecule, surrounded by a solution of its substrates, possibly involving the track. Under specified relations between the concentration of the substrates [18], two independent stationary (nonequilibrium) molar concentrations of the products $[P_1]$ and $[P_2]$, related to the enzyme total concentration $[E]$, are to be treated, respectively, as the input and output dimensionless thermodynamic variables X_1 and X_2 considered in Fig. 1. The fluxes J_i with the conjugate thermodynamic forces A_i are determined as [22]

$$J_i := \frac{d[P_i]}{dt[E]}, \quad \beta A_i := \ln \frac{[P_i]^{\text{eq}}[R_i]}{[R_i]^{\text{eq}}[P_i]}. \quad (1)$$

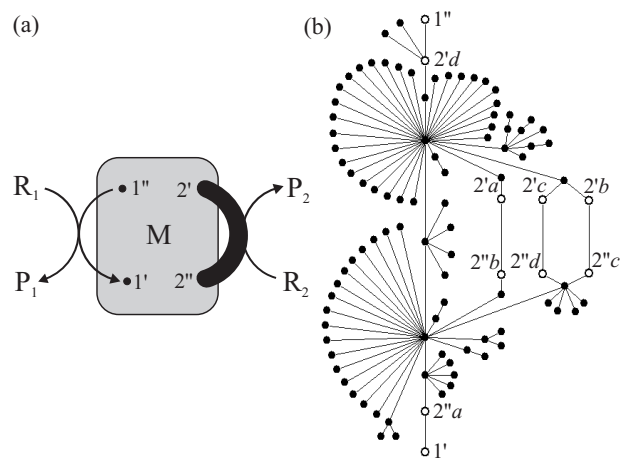


FIG. 2. Kinetics of the enzymatic chemo-chemical machine. (a) General scheme. The gray box represents an arbitrary network of transitions between conformational states composing either the enzyme or the enzyme-substrates native state. All these transitions satisfy the detailed balance condition. A single pair (the ‘gate’) of conformational states $1''$ and $1'$ is distinguished, between which the input reaction $R_1 \leftrightarrow P_1$ brakes the detailed balance. Also, a single or a variety (the heavy line) of pairs of conformational states $2''$ and $2'$ is distinguished, between which the output reaction $R_2 \leftrightarrow P_2$ does the same. All the reactions are reversible; the arrows indicate the directions assumed to be forward. (b) Exemplifying realization of the 100-node network, constructed stochastically following the algorithm described in the Appendix. Note two hubs, the states of the lowest free energy, that can be identified with the two main conformations of the protein machine, e.g., ‘open’ and ‘closed’, or ‘bent’ and ‘straight’, usually the only occupied sufficiently high to be notable under equilibrium conditions. The single pair of the output transition states chosen for the simulations is $(2''a, 2'd)$. The alternative four output pairs $(2''a, 2'a)$, $(2''b, 2'b)$, $(2''c, 2'c)$, and $(2''d, 2'd)$, are chosen tendentially to lie one after another.

$\beta = 1/k_B T$, where k_B is the Boltzmann constant, and the superscript eq denotes the corresponding equilibrium concentrations.

On the mesoscopic level, the dynamics of a particular biological chemo-chemical machine is the Markov process described by a system of master equations, determining a network of conformational transitions that satisfy the detailed balance condition, and a system of pairs of distinguished states (the ‘gates’) between which the input and output chemical reactions force transitions, that break the detailed balance [17, 18] (Fig. 2a). Recently, we proved analytically [18] that, for a single output gate, when the enzyme has no opportunity for any choice, the ratio J_2/J_1 cannot exceed one. This case also includes the various ratchet models, that assume the input and output gates to coincide [8], and for which, consequently, the flux $A_2(J_2 - J_1)$ is non-negative, hence resulting in the entropy increase. The output flux J_2 can only exceed the input flux J_1 in the case of many different output gates.

Our goal is to consider the biological molecular machines with such dynamics. However, very poor experimental support is available for actual conformational transition networks in native proteins [26]. That is why we restrict our attention to a model network here. In Ref. [18], we set a hypothesis that the protein conformational transition networks, like the higher level biological networks, the protein interaction network and the metabolic network, have also evolved in the process of a self-organized criticality [27]. Such networks are scale-free and display a transition from the fractal organization on the small length-scale to the small-world organization on the large length-scale [21]. We have shown [18] that the case of many different output gates is reached in a natural way on scale-free fractal trees, extended by long-range shortcuts. A network of 100 nodes with such properties is depicted in Fig. 2b. Its construction and dynamics is described in the Appendix.

IV. GENERALIZED FLUCTUATION THEOREM

In the mesoscopic machines, the work, dissipation and heat are fluctuating variables and their variations, proceeding forward and backward in time, are related to each other by the fluctuation theorem [28, 29]. The probability distribution function for the input and output fluxes, in general, depending on the time period t of determination, satisfies the stationary fluctuation theorem in the Andrieux-Gaspard form [30]:

$$\frac{p(j_1(t), j_2(t))}{p(-j_1(t), -j_2(t))} = \exp \beta [A_1 j_1(t) + A_2 j_2(t)] t. \quad (2)$$

This can be equivalently rewritten as the Jarzynski equality [28]

$$\langle \exp(-\sum_i \beta A_i \mathcal{J}_i(t)) \rangle = \langle \exp(-\sigma) \rangle = 1. \quad (3)$$

p is the joint probability distribution function for the statistical ensemble of the fluxes, and $\langle \dots \rangle$ is the average over that ensemble. $\mathcal{J}_i(t)$ denotes the random variable of the mean net flux over the time period t , $i = 1, 2$, and $j_i(t)$ denotes the particular value of this flux with J_i in Fig. 1 being the corresponding value for $t \rightarrow \infty$. σ has the meaning of a fluctuating dimensionless entropy production, and the Jensen inequality [28, 29]

$$\langle \exp(-\sigma) \rangle \geq \exp\langle -\sigma \rangle \quad (4)$$

provides the second law of thermodynamics,

$$\langle \sigma \rangle \geq 0, \quad (5)$$

to be a consequence of (3).

From the point of view of the output force A_2 , subsystem 1 carries out work on subsystem 2 while subsystem 2 carries out work on the environment. Jointly, the effective work $A_2(J_2 - J_1)$ is performed on or by subsystem

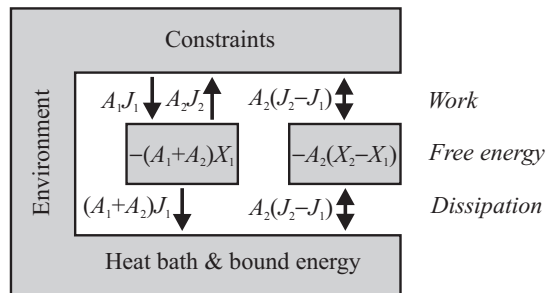


FIG. 3. Alternative view of energy processing in the stationary isothermal machine. Here both the thermodynamic variables X_1 and $X_2 - X_1$ are energetically independent. We still study the direction of the flux denoted by the forward-reverse arrow.

2. The energy processing from Fig. 1 can be alternatively presented as in Fig. 3, with the free energy transduction path absent. Here, the subsystems described by the two variables X_1 and $X_2 - X_2$, respectively, are energetically independent. However, like the subsystems described by the two variables X_1 and X_2 , they are still statistically correlated, what can be checked by considering the two-dimensional probability distribution function $p(j_1, j_2)$ as a two-dimensional probability distribution function $p(j_1, j_2 - j_1)$ with $j_2 - j_1$ treated, as a whole, the single variable.

From the fluctuation theorem (2) for the total entropy production in both the fluxes j_1 and j_2 , the generalized fluctuation theorems for j_1 and the difference $j_2 - j_1$ follow in the logarithmic form:

$$\ln \frac{p(j_1)}{p(-j_1)} = \beta(A_1 + A_2)j_1 t + \beta A_2(J_2 - J_1)t \quad (6)$$

$$+ \int d(j_2 - j_1) p(j_2 - j_1) \ln \frac{p(-j_2 + j_1 | -j_1)}{p(j_2 - j_1 | j_1)}$$

and

$$\ln \frac{p(j_2 - j_1)}{p(-j_2 + j_1)} = \beta A_2(j_2 - j_1)t + \beta(A_1 + A_2)J_1 t \quad (7)$$

$$+ \int dj_1 p(j_1) \ln \frac{p(-j_1 | -j_2 + j_1)}{p(j_1 | j_2 - j_1)},$$

respectively. We introduced conditional probabilities and omitted t for brevity. The Jarzynski equalities corresponding to (6) and (7) can be written as [19, 20, 31]

$$\langle \exp(-\sigma - \iota) \rangle = 1. \quad (8)$$

As in (3), σ has the meaning of a dimensionless entropy production, now only in the flux j_1 or $j_2 - j_1$, but the interpretation of ι is not so easy.

The problem is that for the stationary processes, as opposed to the transient nonequilibrium protocols considered in Refs. [19, 20, 31], the notion of the mutual information is not well defined [32]. Only upon neglecting the two last terms in Eq. (6) for the flux j_1 ,

$$\ln \frac{p(j_1)}{p(-j_1)} \approx \beta(A_1 + A_2)j_1 t, \quad (9)$$

Eq. (7) for the flux $j_2 - j_1$ can be rewritten in terms of the mutual information differences:

$$\ln \frac{p(j_2 - j_1)}{p(-j_2 + j_1)} \approx \beta A_2 (j_2 - j_1) t \quad (10)$$

$$+ \int dj_1 p(j_1) \left[\ln \frac{p(-j_1 | -j_2 + j_1)}{p(-j_1)} - \ln \frac{p(j_1 | j_2 - j_1)}{p(j_1)} \right].$$

Approximation (9) is a type of asymmetrical coarse graining [32] that separates both the fluxes $j_2 - j_1$ and j_1 . Like the antecedent entropic term, the fluctuating integral in Eq. (10) depends only on a single variable $j_2 - j_1$. The integral has the direct interpretation of the information production in nats (the natural logarithm is used instead of the binary logarithm). We leave this name for ι represented by the two last components in the exact relations (6) and (7).

A consequence of (8) is, following the corresponding Jensen inequality, a generalized version of the second law of thermodynamics [19, 20, 31–34]

$$\langle \sigma \rangle \geq -\langle \iota \rangle. \quad (11)$$

In itself alone, the inequality (11) is not very revealing, as it determines the entropy production in one selected thermodynamic variable when the other is hidden [31, 32, 34–36]. Only when $\langle \sigma \rangle$ and $\langle \iota \rangle$ are of the opposite sign, and the latter is positive (an information creation), the entropy production $\langle \sigma \rangle$ is negative, which describes the case of Maxwell’s demon exactly.

We performed Monte Carlo simulations of random walk, described by the respective master equations (see the Appendix), on the network presented in Fig. 2b, with both the single and the fourfold output gate. Exemplifying two-dimensional probability distribution functions of the two fluxes, $p(j_1(t), j_2(t))$, are depicted and discussed in Fig. 8 in the Appendix. Upon analyzing the results we found that:

- (i) The two-dimensional probability distribution function $p(j_1(t), j_2(t))$ satisfies the Andrieux-Gaspard fluctuation theorem (2) for t longer than the mean first passage time between the most distant nodes.
- (ii) The logarithm of the marginal ratio $p(j_1)/p(-j_1)$ can be described by the generalized fluctuation theorem formula (6) with both the entropic and informative components linearly depending on j_1 . The informative correction is, for the conditions assumed, negative and small.
- (iii) the logarithm of the diagonal marginal ratio $p(j_2 - j_1)/p(-j_2 + j_1)$ can be described by the generalized fluctuation theorem formula (7) with both the entropic and informative components linearly depending on the difference $j_2 - j_1$. The informative correction can be of arbitrary sign and large.

The generalized fluctuation theorem dependences of $\ln[p(j_2 - j_1)/p(-j_2 + j_1)]$ are depicted in Fig. 4 for a

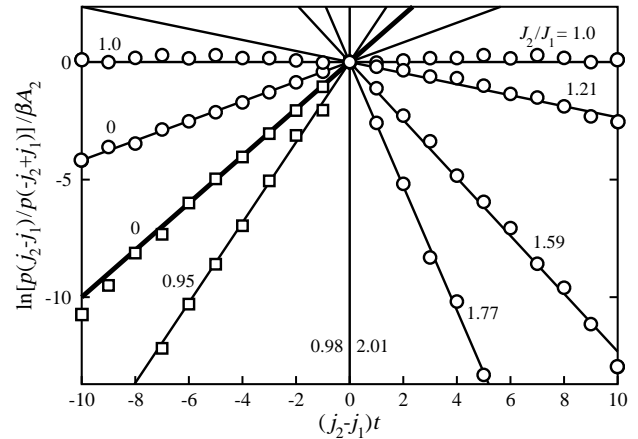


FIG. 4. Generalized fluctuation theorem dependence (7) found in the model random walk simulations. The examined network was that shown in Fig. 2b with the single output gate (the squares) and the fourfold output gate (the circles). The dynamics of the model was described in the Appendix. We assumed $\beta A_1 = 1$ and a few negative values of βA_2 determining the difference $J_2 - J_1$ of the average output and input fluxes (or the ratio J_2/J_1 noted in the figure). The results of each simulation were obtained symmetrically on the whole axis of the fluctuating difference $j_2 - j_1$ but in the figure, they are presented, divided by the (negative!) coefficient βA_2 , only on the left from zero for the negative average $J_2 - J_1$, and on the right from zero for the positive average $J_2 - J_1$. The thick, solid line corresponds to the lack of information transfer in Eq. (7). The such case takes place for the force $\beta A_2 = -0.670$, that stalls the flux through the single output gate ($J_2/J_1 = 0$). The same effect of stalling the flux through the fourfold output gate is reached for $\beta A_2 = -0.173$, but this results in a non-zero information gain (the line with a lower slope). The entropy production is completely compensated for by the information gain for $\beta A_2 = -0.108$, when the average difference $J_2 - J_1$ reaches the value of 0 (the horizontal line). The vertical line ($\beta A_2 = 0$) corresponds to the maximum value of J_2/J_1 both for the fourfold and the single output gate.

few chosen negative values of βA_2 that determine the average difference $J_2 - J_1$ (or the ratio J_2/J_1) of the output and input fluxes. The simulation data are presented in such a way that the transition from the entropy production to entropy reduction might be clearly seen. The thick, solid line corresponds to the first, entropic term to the right-hand side of Eq. (7). We see that the correction, originating from the informative terms, can be very large indeed. For the single output gate, when the system has no opportunity of any choice, this correction is zero or of the same sign as the entropic contribution (positive), that corresponds to an information lost rather than creation. For many output gates, information gain, resulting from the possibility of a choice, reduces the effects of the entropy production in part, until the limit of the tight coupling, $J_2 - J_1 = 0$ ($J_2/J_1 = 1$), above which information creation prevails.

Fig. 4 shows clearly that, for many output gates, the information creation is always of the opposite sign to the entropy production. Note that for $J_2/J_1 > 1$ and for negative βA_2 , the average of the entropic term in Eq. (7) is negative, that corresponds to the entropy reduction. The average dimensionless entropy production (the partial dissipation, divided by $k_B T$) $\beta D = \langle \sigma \rangle$, and the average information creation $I = \langle \iota \rangle$, obtained from the data in Fig. 4, are presented in Fig. 5 as functions of $J_2 - J_1$.

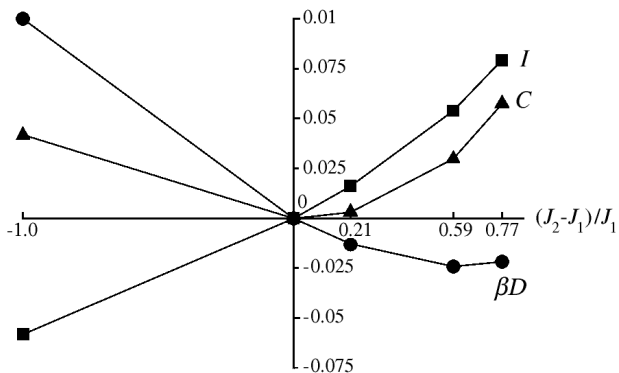


FIG. 5. Dependence of the information creation I and the entropy production βD per $t = 10^3$ random walking steps of determination, on the average difference $J_2 - J_1$. The points represent the values obtained from the data given in Fig. 4. The sum of βD and I , we refer to as the cost C , is also shown (see the discussion in the next Section).

V. ENERGY VERSUS ORGANIZATION PROCESSING

We studied the fluctuations of the flux difference $J_2 - J_1$, which is the time derivative of the variable $X_2 - X_1$. Though involved in the work performance, this variable characterizes not the energy but the organization of the system. In the case of the macroscopic mechanical machines, it could be, for example, the slipping angle of a component wheel to axle. In the case of the macroscopic electrical machines, it could be the variable charge of a component capacitor or battery. The main conclusion of the study is that the free energy processing has to be distinguished from the organization processing (Fig. 6). Note that both the free energy $-A_1 X_1 - A_2 X_2$ and the organization $X_2 - X_1$ are functions of the state of the system.

For the systems operating under stationary isothermal conditions, the first and second laws of thermodynamics

$$W = D \geq 0 \quad (12)$$

are fulfilled for the free energy processing. Both the entire work W and dissipation D are functions of the process (Fig. 3). For the organization processing, the generalized first and second laws can be written as

$$C = \beta D + I \geq 0. \quad (13)$$

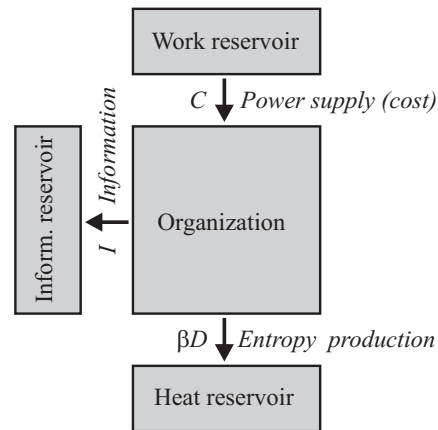


FIG. 6. Organization processing in the system participating in a stationary isothermal process. See the text for the detailed discussion.

Here, both the entropy production βD , the information I , as well as C , the quantity which balances the two former quantities and which could be referred to as the entire cost of the process, are also functions of that process.

For the macroscopic machines as well as the mesoscopic enzymatic machines with a single output gate, the information I and the entropy production βD must always be of the same sign thus positive. Accordingly, I is to be interpreted as the information lost. However, for some enzymatic machines with multiple output gates, we showed here that I , though also positive, must be of the opposite sign to βD , which can be thus negative (the entropy reduction instead of production). Then, I should be interpreted as the information creation rather than lost. Only such biological molecular machines may be said to act as Maxwell's demons. In general, from the point of view of the organization processing, Maxwell's demon is a physical system complex enough to make a choice and to create information. So is also any system that experiences symmetry breaking [37] and, in particular, any quantum system with 'pointer' states, entangled with the rest of the Universe including an observer [38].

When considering the coupling of the free energy donating-process with the free energy-accepting one, the case of the tight coupling, $J_2 - J_1 = 0$, is exceptional. Our simulation clearly points out that such a case happens not for the lack of shortcuts for the fluxes, but for the compensation of the entropy production βD by the information creation I , albeit, on the average, both tend then to zero (compare Fig. 5). This case is the optimum in the sense that the organization cost C of the total process is than zero. We cannot, however, forget that from the energetic point of view, the dissipation $(A_1 + A_2)J_1$ still occurs and it is related with the performance of the work $A_2 J_1$ (unless $A_2 = -A_1$, what takes place for the maximally efficient machine).

Note that we do not distinguish the operating system

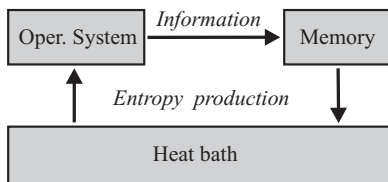


FIG. 7. Transfer of information and entropy production in the operating system and the memory as seen from the point of view of the organization processing.

and the memory as the previous investigators [19, 20, 32–34] did after the Szilard understanding of Maxwell’s demon [2]. Our model describes the action of the autonomous Maxwell demon without necessity of the operating system and the memory determination. However, depending on the context, Fig. 6 can represent also the action of either the very operating system (the nonautonomous Maxwell’s demon) [33], the memory, or both (the autonomous Maxwell’s demon with such division).

The case of the tight coupling occurs in a natural way in systems composed of the operating system and a memory, between which a feedback control [4, 19, 20, 32–34] is realized. From the point of view of the organization processing, both subsystems represent some constraints to one another. No net information creation to environment is necessary, $I = 0$. Transfer of information from the operating system to memory is simultaneously the measurement and the control process. The result is an entropy reduction of the operating system, that can be used for some work performance, and, simultaneously, the equal entropy production in memory, that, following the Landauer theorem [3], must be erased at the expense of the same amount of work. No net entropy production takes place, $\beta D = 0$ (Fig. 7).

VI. BIOLOGICAL IMPLICATIONS

As mentioned earlier [18], our approach is able to explain the observation that the single myosin II head can take several steps along the actin filament per ATP molecule hydrolyzed [24, 25]. It is likely that the mechanism of the action of the small G-proteins that have a common ancestor with the myosin [39] and an alike partly disordered structure after binding the nucleoside triphosphate [40, 41] is, after a malignant transformation, similar. Presumably, also, natively disordered transcription factors [43] actively look [44, 45] and not passively for their target on the genome.

There are convincing arguments, for instance, for the kinesin motor [46, 48, 49], the cytoplasmic dynein motor [50, 51], and the quinol:cytochrome c oxidoreductase [52], that a feedback control with the net $I = 0$ and $\beta D = 0$ is achieved in dimeric protein complexes, which are composed of two identical monomers, simultaneously playing the role of the observer (memory) and the con-

trolled unit. Because of the monomers’ interaction, it is an open question whether the roles of the controlling and the controlled unit can be separated as in the bipartite structures [31, 32, 34], and the formal description of dimeric as well as higher organized protein machines needs more detailed research, when the organization processing is to be taken into account.

ACKNOWLEDGEMENTS

MK thanks Yaşar Demirel and Hervé Cailleau for discussing the problem in the early stages of the investigation.

APPENDIX: METHODS

The algorithm of constructing the stochastic scale-free fractal trees was adopted after Goh et al. [53]. Shortcuts, though more widely distributed, were considered by Rozenfeld, Song and Makse [21]. Here, we chose randomly three shortcuts from the set of all the pairs of nodes distanced by six links. The network of 100 nodes in Fig. 2b is too small to determine its scaling properties, but a similar procedure of construction applied to 10^5 nodes results in a scale-free network that is fractal on a small length-scale and a small world on a large length-scale.

To provide the network with stochastic dynamics, we assumed the probability of changing a node to any of its neighbours to be the same in each random walking step. Consequently, the transition probability to the neighbouring node is inversely proportional to the number of links (the output node degree) and equals $(\tau_{\text{int}} p_i^{\text{eq}})^{-1}$ [18], where p_i^{eq} denotes the equilibrium occupation probability of the exit node. Following the detailed balance condition, the free energy of a given node is proportional to its degree. The most stable conformational substates are the hubs. The mean internal transition time between the neighbouring nodes, τ_{int} , is determined by the doubled number of links, i.e., $2(100 - 1 + 3) = 204$ random walking steps for the 100 node tree network with 3 shortcuts assumed. The mean first passage time between the most distant nodes we found to equal approximately 710 random walking steps.

The forward external transition probabilities, determined by the stationary concentrations $[P_i]$, were assumed to equal $(20 p_i^{\text{eq}})^{-1}$ per random walking step, p_i^{eq} denoting the equilibrium occupation probability of the initial input or output node, $i = 1, 2$. The corresponding backward external transition probabilities were modified by the detailed balance breaking factors $\exp(-\beta A_i)$. The mean forward external transition time $\tau_{\text{ext}} = 20$ is one order of the magnitude shorter than the mean internal transition time between the neighbouring nodes $\tau_{\text{int}} = 204$, so that the whole process is controlled by the internal and not by the external dynamics of the system.

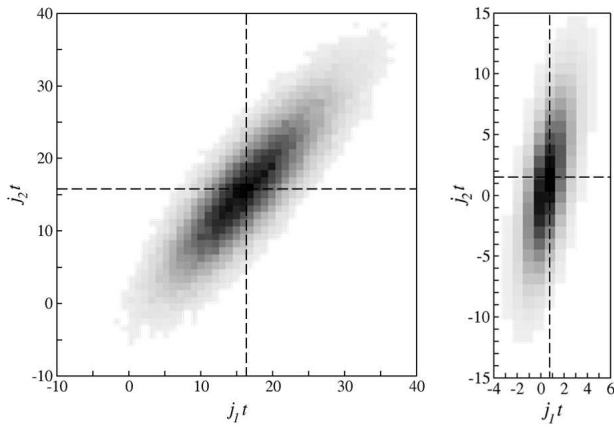


FIG. 8. Exemplifying two-dimensional probability distribution functions $p(j_1(t), j_2(t))$ found in the model random walk simulations on a network with the single output gate (left) and the fourfold output gate (right). For the single output gate, we assumed $t = 10^4$ random walking steps and $J_2/J_1 = 0.95$. For the fourfold output gate, we assumed $t = 10^3$ random walking steps and $J_2/J_1 = 1.59$. The averaged values of the fluxes, multiplied by the time t of determination, are marked by the broken lines. For more details, see the text.

We performed Monte Carlo simulations of the random walk in 10^{10} computer steps on the network shown in Fig. 2b with both the single and the fourfold output gate. The gates were chosen tendentiously to maximize the value of J_2/J_1 . To get the statistical samples of the fluxes numerous enough, we chose the time of averaging $t = 10^4$ random walking steps for the single gate and $t = 10^3$ random walking steps for the fourfold gate. Exemplary two-dimensional probability distribution functions $p(j_1(t), j_2(t))$ are shown in Fig. 8. Instead of the orthogonal coordinates (j_1, j_2) , the skew coordinates $j_1, j_2 - j_1$ were considered and from the two-dimensional distributions $p(j_1, j_2 - j_1)$, the diagonal marginals $p(j_2 - j_1)$ were determined. We discarded the rare results for the higher values of $j_2 - j_1$ as being burdened with statistical error too large. However, it is planned to investigate in more detail the tails of the distribution $p(j_2 - j_1)$ in future, as effects of a nonlinear dependence are expected [36].

-
- [1] J. C. Maxwell, *Theory of Heat* (Logmans, London, 1871).
[2] L. Z. Szilard, *Z. Phys.* **53**, 840 (1929).
[3] H. S. Leef and A. F. Rex, eds., *Maxwell's Demon 2: Entropy, Classical and Quantum Information, Computing* (Institute of Physics Publishing, Philadelphia, 2003).
[4] Z. Lu, D. Mandal, and C. Jarzynski, *Physics Today* **67**, 60 (2014).
[5] M. Smoluchowski, *Phys. Z.* **13**, 1069 (1912).
[6] R. P. Feynman, R. B. Leighton, and M. Sands, *The Feynman Lectures on Physics*, vol. 1 (Addison-Wesley, Reading, 1963), chap. 46.
[7] A. F. Huxley, *Prog. Biophys. Biophys. Chem.* **7**, 255 (1957).
[8] J. Howard, in *Biological Physics - Poincaré Seminar 2009*, B. Duplainer and V. Rivasseau, eds. (Springer, Basel, 2010), pp 47-61.
[9] M. Kurzynski, *Prog. Biophys. Molec. Biol.* **69**, 23 (1998).
[10] M. A. Fisher and A. B. Kolomeisky, *Proc. Natl. Acad. Sci. USA* **96**, 6597 (1999).
[11] A. B. Kolomeisky and M. E. Fisher, *Annu. Rev. Phys. Chem.* **58**, 675 (2007).
[12] D. Tsygankov and M. E. Fisher, *J. Chem. Phys.* **128**, 015102 (2008).
[13] R. D. Astumian and I. A. Derenyi, *Biophys. J.* **77**, 993 (1999).
[14] B. Bustamante, D. Keller, and G. Oster, *Acc. Chem. Res.* **34**, 412 (2001).
[15] R. Lipowsky, *Phys. Rev. Lett.* **85**, 4401 (2000).
[16] R. Lipowsky, S. Liepelt, and A. Valleriani, *J. Stat. Phys.* **135**, 951 (2009).
[17] M. Kurzynski and P. Chelminiak, *J. Stat. Phys.* **110**, 137 (2003).
[18] M. Kurzynski, M. Torchala, and P. Chelminiak, *Phys. Rev. E* **89**, 012722 (2014).
[19] T. Sagawa and M. Ueda, *Phys. Rev. E* **85**, 021104 (2012).
[20] T. Sagawa and M. Ueda, *Phys. Rev. Lett.* **109**, 180602 (2012).
[21] H. D. Rozenfeld, C. Song, and H. A. Makse, *Phys. Rev. Lett.* **104**, 025701 (2010).
[22] T. L. Hill, *Free Energy Transduction and Biochemical Cycle Kinetics* (Springer, New York, 1989).
[23] M. Kurzynski, *The Thermodynamic Machinery of Life* (Springer, Berlin, 2006).
[24] K. Kitamura, M. Tokunaga, A. H. Iwane, and T. Yanagida, *Nature* **397**, 129 (1997).
[25] K. Kitamura, M. Tokunaga, S. Esaki, A.-H. Iwane, and T. Yanagida, *Biophysics* **1**, 1 (2005).
[26] K. Henzler-Wildman and D. Kern, *Nature* **450**, 964 (2007).
[27] K. Sneppen and G. Zocchi, *Physics in Molecular Biology* (Cambridge University Press, New York, 2005), chaps. 8 and 9.
[28] C. Jarzynski, *Eur. Phys. J. B* **64**, 331 (2008).
[29] U. Seifert, *Rep. Prog. Phys.* **75**, 126001 (2012).
[30] D. Andrieux and P. Gaspard, *J. Stat. Phys.* **127**, 107 (2007).
[31] N. Shiraiishi and T. Sagawa, *Phys. Rev. E* **91**, 012130 (2015).
[32] J. M. Horowitz and M. Esposito, *Phys. Rev. X* **4**, 031015 (2014).
[33] S. Deffner and C. Jarzynski, *Phys. Rev. X* **3**, 041003 (2013).
[34] D. Hartich, A. C. Barato, and U. Seifert, *J. Stat. Mech.* **14**, P02016 (2014).
[35] J. Mehl, B. Lander, C. Bechinger, V. Blickle, and U. Seifert, *Phys. Rev. Lett.* **108**, 220601 (2012).

- [36] M. Borrelli, J. V. Koski, S. Maniscalco, and J. P. Pekola, *Phys. Rev. E* **91**, 012145 (2015).
- [37] P. W. Anderson, *Science* **177**, 393 (1972).
- [38] W. H. Zurek, *Revs Mod. Phys.* **75**, 715 (2003).
- [39] F. J. Kull, R. D. Vale, and R. J. Fletterick, *J. Muscle Res. Cell Motil.* **19**, 877 (1998).
- [40] H. Houdusse, H. L. Szent-Györgi, and C. Cohen, *Proc. Natl. Acad. Sci. USA* **97**, 11238 (2000).
- [41] I. Kosztin, R. Bruinsma, P. O’Lague, and K. Schulten, *Proc. Natl. Acad. Sci. USA* **99**, 3575 (2002).
- [42] M. Slutsky and L. A. Mirny, *Biophys. J.* **87**, 4021 (2004).
- [43] A. Tafvizi, F. Huang, A. R. Ferhst, L. A. Mirny, and A. M. A. van Oijen, *Proc. Natl. Acad. Sci. USA* **108**, 263 (2011).
- [44] G. M. Viswanathan, A. Afanasyev, S. V. Buldyrev, S. Havlin, M. G. E. da Luz, E. P. Raposo, and H. E. Stanley, *Physica A* **282**, 1 (2000).
- [45] G. M. Viswanathan, E. P. Raposo, and M. G. E. da Luz, *Phys. Life Revs.* **5**, 133 (2008).
- [46] M. Bier, *Biosystems* **88**, 301 (2007).
- [47] R. D. Astumian, *Biosystems* **93**, 8 (2008).
- [48] S. Liepelt and R. Lipowski, *Phys. Rev. E* **79**, 011917 (2009).
- [49] R. D. Astumian, *Biophys. J.* **98**, 2401 (2010).
- [50] D. Tsygankov, A. W. R. Serohijos, N. V. Dokholyan, and T. C. Elston, *J. Chem. Phys.* **130**, 025101 (2009).
- [51] D. Tsygankov, A. W. R. Serohijos, N. V. Dokholyan, and T. C. Elston, *Biophys. J.* **101**, 144 (2011).
- [52] M. Świerczek, E. Cieluch, M. Sarewicz, A. Borek, C. C. Moser, P. L. Dutton, and A. Osyczka, *Science* **329**, 451 (2010).
- [53] K.-I. Goh, G. Salvi, B. Kahng, and D. Kim, *Phys. Rev. Lett.* **96**, 018701 (2006).